Comparing Rupture Velocities in Small and Large Earthquakes
2004 SCEC FINAL REPORT

Jeff McGuire
Woods Hole Oceanographic Institution

The goal of this proposal was to begin constraining the rupture velocity, v_r, of small earthquakes on important seismogenic faults in Southern California. This is a vital yet essentially unknown quantity in earthquake physics. It's importance lies in being a macroscopic observable that is directly connected to the microscopic physics during rupture. In large earthquakes, ruptures propagate close to (or above) the theoretical limiting speed, a well established observation which implies that a relatively small fraction of the available energy is used to create new fractures. This is not unexpected given that laboratory estimates of the critical slip distance over which friction decays from "static" to "dynamic" values are many orders of magnitude smaller than the slip in large earthquakes (i.e. microns vs meters). By constraining the rupture velocity of earthquakes that only slip a cm or less, I want to constrain the frictional weakening process at a scale that is unobservable in complicated large earthquakes owing to the filtering/smoothing in those inversions. Determining the influence of fracture energy in small earthquakes has traditionally been attempted by quantifying the scaling of radiated energy (E) with seismic moment. This is actually a harder problem to solve, resulting in order of magnitude uncertainties in the important quantity (E), because it requires correcting for propagation effects up to higher frequencies and for rupture kinematic effects. This approach has yet to yield a widely accepted determination of whether the ratio of radiated energy to seismic moment changes systematically with earthquake size in part because of the difficulties in correcting for propagation at high frequencies. The radiated energy measurement is concentrated in the frequency band from about the earthquake's corner frequency up to about a factor of five to ten higher in frequency (say 10-100 Hz for a magnitude 3.0 earthquake). In contrast, bounds on rupture velocity can be determined from azimuthal variations in the corner frequency (say from 7-15 Hz for the same magnitude 3.0 earthquake with a duration of ~.1 seconds).

Determining the rupture velocity of small earthquakes on real faults is difficult because the far-field seismograms typically available for such earthquakes in practice do not allow a unique determination of a densely parameterized finite-fault model that is relatively free from imposed assumptions about slip/rupture evolution (Venkataraman, Mori et al. 2000). The simplest parameterization of an earthquake rupture that contains information about the rupture propagation without imposing any a priori physical model on a particular earthquake is known as the second moments (or variances) of the rupture which measure the length, width, duration, and directivity in a weighted average sense (Backus and Mulcahy 1976a, Backus and Mulcahy 1976b; Backus 1977a; Backus 1977b; McGuire, Zhao et al. 2001; McGuire, Zhao et al. 2002). The six parameters that need to be estimated to determine the second moments are linearly related to the variances, $\mu_s^{(0,2)}$, of the Apparent Source Time Functions (ASTF) that result from standard Empirical Green's Function (EGF) deconvolutions (McGuire 2003). Thus, the most straightforward way to infer information about the spatial extent and rupture propagation of small (magnitude ~3-5) earthquakes is to perform the standard EGF analysis, but then interpret the azimuthal variation in the duration of the resulting time functions in terms of the second moments.

Figure 1 shows an example of this measurement for a magnitude 3.0 event at Parkfield recorded by the Berkeley HRSN and a temporary PASSCAL deployment for SAFOD. The stations to the NW of the event showed relatively long duration time functions (about .11 to .13 seconds) while the stations to the southeast showed relatively short time functions (about .06 to .09 seconds). These ASTF durations were inverted for the second moments of the slip distribution, and the results correspond to a characteristic rupture length of about 280 m, a duration of about .10 seconds, a directivity ratio of about .7 indicating a predominately unilateral rupture to the SE, and a "average velocity of the instantaneous centroid", v_0, (see Backus 1977a,b) of about 1.7 km/s. For ruptures with directivity ratios significantly less than 1.0, v_0 gives a lower bound on the rupture velocity (McGuire 2003). Hence, the second moments indicate that this magnitude 3.0 event had a rupture velocity larger than about 0.5 times the shear-wave speed (given a source depth of ~10 km with Vs~3.6 km/s). This estimate is only a lower bound because the event was not purely unilateral (i.e. directivity ratio of 1.0).

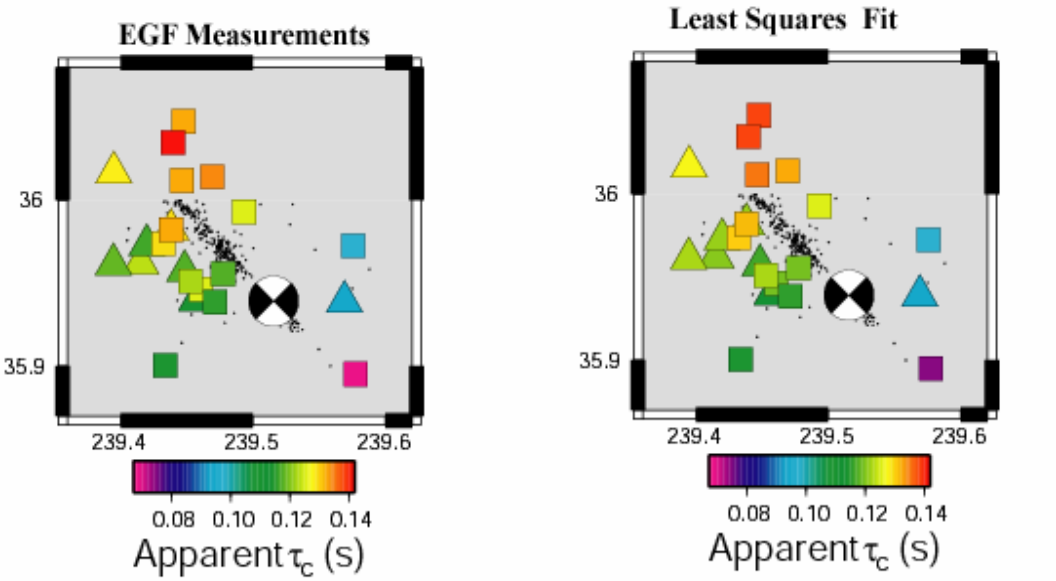

Figure 1. In August of 2002, a M3.0 earthquake occured at 10 km depth in the middle of the Parkfield HRSN and a PASSCAL deployment to monitor the SAFOD site. The high SNR and on-scale recordings of this event and a magnitude 1.3 aftershock provide one of the best availible datasets for studying rupture velocity of small earthquakes. Both the P (triangles) and S (squares) waves show a clear azimuthal patterrn of long apparent duration (τ_c) RSTFs at stations to the northwest and short apparent durations (τ_c) at stations to the southeast. This signal is charachteristic of a nearly unilateral rupture to the southeast similar to the directivity in the M6 earthquakes in this area. The Least squares inversion with the non-negative volume constraint results in best estimates of L_c=280 m, W_c=150 m, a directivity ratio of 0.7, and τ_c of .11 s, and a v_0 of 1.7 km/s to the southeast. The apparent τ_c estimates at essentialy adjacent stations are consistent to within .0033 seconds allowing us to use this level of misfit as an upper bound on the range of acceptable solutions.

The value of v_0 observed at Parkfield is lower than I found for a similar magnitude 3.0 quake that occurred further north on the SAF in the creeping section and was recorded by a PASSCAL array. For that purely unilateral rupture (directivity ~.99) the rupture velocity estimate was about 2.0-2.2 km/s (McGuire 2003), which corresponded to a velocity of about 0.8 of the shear wave speed (~2.4-3.0 km/s) owing to

the events shallower depth (3 km). This pair of San Andreas events illustrate the dangers in forcing a parameterization (such as a Haskell rupture) on even an event with clear directivity. Moreover, they demonstrate the need for an approach that places quantitative error bounds on average rupture velocity that are independent of model assumptions (i.e. a circular crack or Haskell type rupture). It appears that really small values of v_r (i.e. say less than ~.5 Vs) can be ruled out for some mode-II ruptures on the SAF at the magnitude 3.0 level. However, much of the interesting debate is in the difference between ruptures that propagate at 0.5 of the shear-wave speed versus those that approach the Rayleigh speed (say about 0.8-0.92 of the shear-wave speed).

The majority of my efforts this year were on making improvements to the inversion scheme that will allow for quantitative constraints on where an earthquake lies in the v_r~0.5 to 0.9 V_s range. Under the assumption of a constant moment-tensor during rupture, the second moments are defined as:

$$\underline{\underline{\mu}}^{(2,0)} = \iint \dot{f}(\underline{r},t)(\underline{r}-\underline{r}_0)(\underline{r}-\underline{r}_0)dVdt \qquad \mu^{(0,2)} = \iint \dot{f}(\underline{r},t)(t-t_0)(t-t_0)dVdt \qquad (1)$$

$$\underline{\mu}^{(1,1)} = \iint \dot{f}(\underline{r},t)(\underline{r}-\underline{r}_0)(t-t_0)dVdt$$

where $\dot{f}(\underline{r},t)$ is a scalar function that describes the spatial and temporal distribution of moment release along the fault [see McGuire et al., 2002], $\underline{r}_0$ is the centroid location, t_0 is the centroid time, and the integrals are taken over the entire source volume and earthquake duration (Backus 1977; Backus 1977; McGuire et al. 2001). The true second moments are linearly related to the duration (i.e. variance) of the ASTF from an EGF deconvolution, $\mu_s^{(0,2)}$ by:

$$\mu_s^{(0,2)} \approx \mu^{(0,2)} - 2\underline{s}\cdot\underline{\mu}^{(1,1)} + \underline{s}^T\cdot\underline{\underline{\mu}}^{(2,0)}\cdot\underline{s}\,, \qquad (2)$$

where $\underline{s}$ is the slowness vector of the P (or S) wave at the source. I typically invert Equation 2, subject to a non-negative volume constraint, for a least-squares estimate of the 6 unique elements of $\underline{\underline{\mu}}^{(2,0)}$, $\mu^{(0,2)}$, and $\underline{\mu}^{(1,1)}$. Since the data are essentially (azimuthally varying) apparent durations of the rupture, this approach often has a moderate tradeoff between the rupture length and the rupture velocity.

One relatively straightforward way to evaluate the magnitude of this tradeoff for a given dataset is to reformulate the inversion to find the values of the second moments that maximize (or minimize) rupture area for a given level of misfit to the data (as defined by equation 2). This is achievable because the rupture area is proportional to the determinant of the second spatial moment. In a principal axes coordinate system, the eigenvalues of $\underline{\underline{\mu}}^{(2,0)}$, are L_c and W_c, the characteristic rupture length and width respectively. Thus by maximimizng (or minimizing) the determinant of $\underline{\underline{\mu}}^{(2,0)}$ for a given misfit level, the tradeoff between rupture area and rupture velocity can be effectively explored. Determinant maximization is a well studied class of optimization algorithms, and we follow the semi-definite programming implementation of Vandenberghe and Boyd (1996). We enforce the misfit criteria using a matrix inequality (Schur complement) representation of equation 2. The result of this new approach, developed this year with SCEC funding, is shown in figure 2. Essentially any value of misfit can be specified, and the maximum and minimum rupture areas (and related velocities and lengths) is determined.

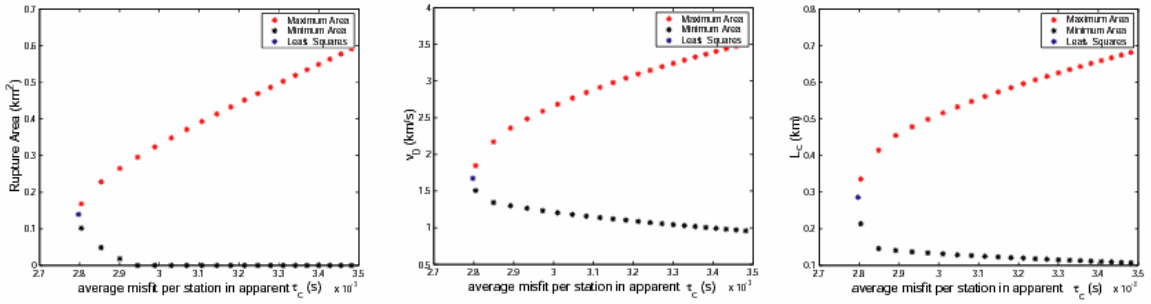

Figure 2. Tradeoff curves of rupture area, v_0, and Lc as a function of the average misfit permitted per station. For each figure, the blue aerik denotes the least-squares solution while the red and black stars denote the values corresponding to the maximum and minimum rupture areas that can be consistent with a given value of misfit (i.e the x axis). Misfits less than about 3 to 3.2 are reasonable from the correlation of measurements at adjacent stations, but the inversions corresponding to these values systematically underestimate the azimuthal variation observed in the apparent durations (Figure 1). The difference between the maximum and minimum rupture area curves results primarily from the difficulty in constraining the rupture width, as the "minimum rupture area" curve rapidly approaches very large aspect ratio (>100) ruptures that are physically unlikely. Thus, any a priori constraint on the aspect ratio essentially places a lower bound on the possible rupture velocity.

I have only recently completed the technique development/implementation stage of this approach, and hence am just beginning to derive scientific results from it. One obvious result in figure 2 is that even with an extremely good station geometry (i.e. Figure 1), the minimum rupture area is very poorly determined. This result occurs because the constraint on the largest eigenvalue of $\underline{\underline{\mu}}^{(2,0)}$ is naturally much better than that on the smallest eigenvalue (i.e. the rupture width). This observation has significant implications for small earthquake stress drop estimates, which inherently depend on rupture width. Estimates of stress drops for small earthquakes range over three orders of magnitude and often approach the theoretical strength of rocks. Much of this is probably a reflection of the leftmost panel of figure 2 which demonstrates that, the minimum rupture width (i.e. maximum stress drop) consistent with a given set of EGF deconvolutions is essentially undetermined for realistic levels of measurement uncertainty. This particular earthquake is a somewhat difficult case because of the large source depth of the event (~10 km, i.e. only a few downgoing rays), but clearly the second moments formulation allows a natural assessment of a seismic network's ability to independently constrain both L_c and W_c, and hence stress drop.

A more optimistic assessment of small earthquake source properties comes from examining the quantities that don't depend on the smallest eigenvalue of $\underline{\underline{\mu}}^{(2,0)}$, most importantly rupture velocity. V_0 is (conservatively) determined to within a factor of two, much better than the order(s) of magnitude uncertainty in E/M. Moreover, this is far from an ideal earthquake because of it's large epicentral depth (10 km) and the very uneven station distribution in the Parkfield region. Much tighter constraints could be placed on a more ideal earthquake (i.e. a purely unilateral event with better station coverage and a larger magnitude difference between the EGF and mainshock, etc).

Attempts to find the best dataset for determining v_r in small earthquakes: I have evaluated several datasets this year for suitability for second moments determination. The San Simeon aftershock dataset (USGS-SCEC) is both promising and problematic as the station distribution is time dependent and vary sparse to the west. There may be a

small time window where M~3 earthquakes have the right recording geometry for second moment determinations. The ANZA array appears to loose clear sensitivity to finite source effects around magnitude 3.5. I will continue to process large ANZA events as they happen, but they are relatively infrequent. Perhaps the most promising dataset so far this year is the Chi-Chi aftershock dataset. Not only is the background station geometry outstanding, but several temporary deployments even improved it. Wu-Cheng Chi (recent Caltech post-doc, and current IES faculty in Taiwan) is visiting WHOI this fall and will be working on this dataset.

Incorporation of 2nd moments results into "LA3D" This fall, I've begun working with Sue Perry and Andrew Hart (a SCEC school year intern at USC) to add the display of 2nd moment derived estimates of rupture area to LA3D. One of the surprising results of my work on 2nd moments in Southern California, is that many of the M~4.5 earthquakes are actually on small conjugate structures rather than the big through going faults (see McGuire SCEC final report 2003). This includes the Yorba Linda earthquake and the 2001 Halloween earthquake on the San Jacinto. By displaying ellipsoidal surfaces that represent the approximate rupture length and width, determined from the second moments inversion, of M~4 earthquakes in LA3D, I hope it will become easier to understand the complicated geometrical structures of fault systems like the San Jacinto that often look like blurry clouds of seismicity when only viewed with earthquake hypocenters. This aspect of my project may be relevant to the structural representation/CFM group depending on the level of detail they seek. Moreover, if the ESP group is going to attempt simulations on a realistic fault structures (e.g. for pathway 3), it will need to know about complicated relay structures at great depth (~10km), like the one that ruptured in the Halloween earthquake within the trifurcation area of the San Jacinto, that are not easily imageable with active source seismics or relative earthquake locations.

References

Backus, G. and M. Mulcahy (1976). " Moment Tensors and Other Phenomenological Descriptions of Seismic Sources-I. Continuous Displacements." Geophys. J. R. astr. Soc. **46**: 341-361.

Backus, G. and M. Mulcahy (1976). " Moment Tensors and Other Phenomenological Descriptions of Seismic Sources-II. Discontinuous Displacements." Geophys. J. R. astr. Soc. **47**: 301-329.

Backus, G. E. (1977). " Interpreting the Seismic Glut Moments of Total Degree Two or Less." Geophys. J. R. astr. Soc. **51**: 1-25.

Backus, G. E. (1977). "Seismic Sources with Observable Glut Moments of Spatial Degree Two." eophys. J. R. astr. Soc. **51**: 27-45.

Kanamori, H. and L. Rivera (2003). "Static and Dynamic Scaling Relations for Earthquakes and Their Implications for Rupture Speed and Stress Drop." Bull. Seism. Soc. Am.: in press.

McGuire, J. J. (2003). "Estimating the finite source properties of small earthquake ruptures." Bull. Seism. Soc. Am., 94, 377-393.

McGuire, J. J., L. Zhao, et al. (2001). " Measuring the second-degree moments of earthquake space-time distributions." Geophys. J. Intl. **145**: 661-678.

McGuire, J. J., L. Zhao, et al. (2002). "Predominance of Unilateral Rupture for a Global Catalog of Large Earthquakes." Bull. Seism. Soc. Am. **92**(8): 3309-3317.

Venkataraman, A., J. Mori, et al. (2000). " Fine structure of the rupture zone of the April 26 and 27, 1997, Northridge aftershocks." J. Geophys. Res. **105**: 19085-19093.